Imaging Science in Dentistry 2022; 52: 171-9
https://doi.org/10.5624/isd.20220025

Effect of different voxel sizes on the accuracy of CBCT measurements of trabecular bone microstructure: A comparative micro-CT study

Mahmure Ayşe Tayman[1], Kıvanç Kamburoğlu[2,*], Mert Ocak[3], Doğukan Özen[4]

[1]*Department of Periodontology, Faculty of Dentistry, Ankara Yıldırım Beyazıt University, Ankara, Turkey*
[2]*Department of Dentomaxillofacial Radiology, Faculty of Dentistry, Ankara University, Ankara, Turkey*
[3]*Department of Basic Medical Sciences-Anatomy, Faculty of Dentistry, Ankara University, Ankara, Turkey*
[4]*Department of Biostatistics, Faculty of Veterinary Medicine, Ankara University, Ankara, Turkey*

ABSTRACT

Purpose: The aim of this study was to assess the accuracy of cone-beam computed tomographic (CBCT) images obtained using different voxel sizes in measuring trabecular bone microstructure in comparison to micro-CT.

Materials and Methods: Twelve human skull bones containing posterior-mandibular alveolar bone regions were analyzed. CBCT images were obtained at voxel sizes of 0.075 mm (high: HI) and 0.2 mm (standard: Std), while micro-CT imaging used voxel sizes of 0.06 mm (HI) and 0.12 mm (Std). Analyses were performed using CTAn software with the standardized automatic global threshold method. Intraclass correlation coefficients were used to evaluate the consistency and agreement of paired measurements for bone volume (BV), percent bone volume (BV/TV), bone surface (BS), trabecular thickness (TbTh), trabecular separation (TbSp), trabecular number (TbN), trabecular pattern factor (TbPf), and structure model index (SMI).

Results: When compared to micro-CT, CBCT images had higher BV, BV/TV, and TbTh values, while micro-CT images had lower BS, TbSp, TbN, TbPf, and SMI values ($P<0.05$). The BV, BV/BT, TbTh, and TbSp variables were higher with Std voxels, whereas the BS, TbPf, and SMI variables were higher with HI voxels for both imaging methods. For each imaging modality and voxel size evaluated, BV, BS, and TbTh were significantly different ($P<0.05$). TbN, TbPf, and SMI showed statistically significant differences between imaging methods ($P<0.05$). The consistency and absolute agreement between micro-CT and CBCT were excellent for all variables.

Conclusion: This study demonstrated the potential of high-resolution CBCT imaging for quantitative bone morphometry assessment. ***(Imaging Sci Dent 2022; 52: 171-9)***

KEY WORDS: X-Ray Microtomography; Cone-Beam Computed Tomography; Trabecular Bone; Mandible

Introduction

Accurate dental implant placement and maintenance of primary implant stability are key factors for sufficient osseointegration and the long-term success of dental implant rehabilitation.[1] Micro-movement caused by primary imbalance of the implant may lead to fibrous tissue formation around the implant, causing loss of osseointegration and implant failure.[2] Bone quality[3] can affect bone resistance to fracture and may be considered as the combination of all bone properties, for which reason it is among the most important factors affecting primary implant stability.[4] Bone mineral density and trabecular microstructure are the most important determinants of bone strength.[5] However, these 2 parameters should be evaluated simultaneously in order to provide a better estimate of bone strength.[6]

Quantitative bone morphometry is the standard method of evaluating trabecular structural features through morphometric indices. Trabecular and cortical bone microarchitecture properties have been investigated by examining

Received February 3, 2022; Revised March 24, 2022; Accepted April 2, 2022
Published online April 28, 2022
*Correspondence to : Prof. Kıvanç Kamburoğlu
Department of Dentomaxillofacial Radiology, Faculty of Dentistry, Ankara University, Emniyet Mahallesi, Mevlana Bulvarı, Sabancı Kız yurdu karşısı/Yenimahalle, Ankara, Turkey
Tel) 90-312-296-5632, E-mail) dtkivo@yahoo.com

Imaging Science in Dentistry · pISSN 2233-7822 eISSN 2233-7830

2-dimensional (2D) sections from bone biopsies with the help of stereological methods.[7] These histological analyses offer high spatial resolution and good image contrast; however, they are time-consuming and labor-intensive. Moreover, these destructive techniques allow tissue measurement of only a limited number of 2D sections.

Due to the anisotropic nature of trabecular bone, various three-dimensional (3D) imaging methods were proposed to overcome some of the limitations of 2D analyses. In recent years, micro-computed tomography (CT) has been recognized as a highly reliable new reference method in *ex vivo* bone studies for determining trabecular bone parameters.[8] However, due to the small scanning area limited to *ex vivo* small bone samples, micro-CT has shown almost no clinical value for structural bone analysis and has not been used for human patients.[9] In comparison to conventional CT, cone-beam computed tomography (CBCT) provides many clinically objective and quantitative benefits for understanding the morphometric characterization of trabecular bone in terms of radiation dose, cost, scanning time, and improved image accuracy. CBCT is now widely used for subjective assessments of alveolar bone density prior to dental implant placement.[10-12]

When compared to micro-CT, which is currently accepted as the gold standard, the 3-dimensional evaluation of trabecular bone on CBCT may be an appropriate validation method. The main disadvantage of CBCT is its low spatial resolution (200-300 mm) when compared to micro-CT.[13] Today, available CBCT devices offer clear improvements in spatial resolution and availability of a wide voxel size range, thereby providing true sharpness at both clinical and technical levels. Although it is assumed that images with voxel sizes larger than 300 mm are not suitable for trabecular imaging,[14] it may be possible to evaluate trabecular morphology using CBCT devices with smaller voxel sizes. It is necessary to investigate to what extent the voxel dimensions of CBCT allow the correct calculation of morphometric indices.

Although some studies have reported high geometric accuracy of CBCT for linear measurement,[15,16] its reliability for bone quality assessment remains unclear. Several studies have suggested that CBCT might be applied to evaluate trabecular bone microstructure.[17,18] However, CBCT is unable to display calibrated voxel gray values expressed as Hounsfield units due to excessive scattering and technology-specific artifacts.[19,20] In addition, X-ray tube settings and the soft tissue surrounding samples may also affect the morphological parameters and associated clinical evaluations of bone structure.

It is important to know the features of the micro-trabecular structure of the mandible in order to determine the ideal implant treatment plan and prognosis. Determining the most effective radiographic method and voxel size for implant treatment planning is crucial in clinical practice. The main purpose of this study was to evaluate the micro-trabecular structure of the mandible using CBCT and micro-CT images obtained at different voxel sizes.

Materials and Methods

Twelve human skulls containing posterior-mandibular alveolar bone regions were included in this *ex vivo* study. The intact alveolar bones had molar and premolar teeth without fillings, pins, wires, or other metal restorations. Ethical approval for this study was obtained from the Ankara University Faculty of Dentistry Clinical Research Ethics Committee (No: 13/01, date: 18.11.2020).

Image acquisition

Before images were taken, the entire mandible was covered with 2 layers of pink wax to simulate soft tissue. For micro-CT, images were obtained using a 68×68 mm field of view (FOV) at 40 kVp and 140 mA using a Super Argus PET/CT device (Sedecal USA Inc., Arlington, VA, USA) with voxel sizes of 0.06 mm (high; HI) and 0.12 mm (standard; Std). The irradiation time was 10 minutes and 30 seconds for the 0.06-mm voxel images and 6 minutes and 45 seconds for the 0.12-mm voxel images. CBCT images were taken using a Planmeca Promax 3D Max device (Planmeca, Helsinki, Finland) with voxel sizes of 0.075 mm (HI) and 0.2 mm (Std). The imaging parameters for images with a voxel size of 0.075 mm (HI) were 96 kVp, 7.1 mA, 15 s, 55×50 mm FOV, and a 657 mGy $\cdot$ cm^2 dose area product (DAP) value. The imaging parameters for images with a voxel size of 0.2 mm (Std) were 10×59 mm FOV, 96 kVp, 5.6 mA, 12 s, and a DAP value of 728 mGy $\cdot$ cm^2.

Both micro-CT and CBCT images were recorded in the Digital Imaging and Communications in Medicine (DICOM) image format and analyzed using the same 3D analysis program. The analyses were performed in CTAn software (CTAnalyser, Kontich, Belgium; version 1.17.7.2; Bruker micro-CT) using the standardized automatic global threshold method. The region of interest was selected in the trabecular bone region between the same teeth and performed by a well-trained and experienced researcher using automatic calibration of the CTAn software. The measurements were repeated twice at a 2-week interval and averaged. The parameters measured were as follows. Bone vol-

Table 1. Descriptive statistics for the measurements and comparison of the average measurements

Paired variables		Mean ± standard deviation	Median (min-max)	*P*-value
Bone volume (BV)	Micro-CT_Std	509.99 ± 279.52	529.12 (150.08-893.74)[d]	< 0.05
	Mcro-CT_HI	500.21 ± 277.90	520.57 (145.37-881.91)[c]	
	CBCT_Std	623.41 ± 318.26	633.68 (222.57-1080.02)[a]	
	CBCT_HI	609.65 ± 313.49	621.48 (214.9-1049.11)[b]	
Percent bone volume (BV/TV)	Micro-CT_Std	46.01 ± 8.48[c]	45.09 (32.7-65.61)	< 0.05
	Mcro-CT_HI	44.28 ± 8.47[b]	44.16 (31.22-64.29)	
	CBCT_Std	57.13 ± 11.10[a]	56.21 (39.46-80.96)	
	CBCT_HI	54.45 ± 11.98[a]	54.85 (33.43-78.35)	
Bone surface (BS)	Micro-CT_Std	2396.02 ± 600.35	2263.13 (1395.14-3652.63)[b]	< 0.05
	Mcro-CT_HI	2448.16 ± 608.05	2278.56 (1409.18-3683.03)[a]	
	CBCT_Std	1841.62 ± 432.16	1766.85 (1099.99-2684.81)[d]	
	CBCT_HI	1890.12 ± 436.09	1827.11 (1104.41-2730.95)[c]	
Trabecular thickness (TbTh)	Micro-CT_Std	0.24 ± 0.06[c]	0.24 (0.17-0.38)	< 0.05
	Mcro-CT_HI	0.23 ± 0.06[d]	0.22 (0.15-0.35)	
	CBCT_Std	0.46 ± 0.09[a]	0.44 (0.33-0.62)	
	CBCT_HI	0.44 ± 0.09[b]	0.42 (0.32-0.61)	
Trabecular separation (TbSp)	Micro-CT_Std	0.53 ± 0.11	0.5 (0.4-0.8)	0.213
	Mcro-CT_HI	0.51 ± 0.11	0.48 (0.4-0.79)	
	CBCT_Std	0.48 ± 0.12	0.47 (0.3-0.68)	
	CBCT_HI	0.46 ± 0.12	0.46 (0.28-0.65)	
Trabecular number (TbN)	Micro-CT_Std	2.05 ± 0.46[a]	2.08 (1.56-2.99)	< 0.05
	Mcro-CT_HI	2.04 ± 0.47[a]	2.08 (1.55-3.04)	
	CBCT_Std	1.43 ± 0.25[b]	1.39 (1.16-2.12)	
	CBCT_HI	1.43 ± 0.29[b]	1.38 (1.15-2.23)	
Trabecular pattern factor (TbPf)	Micro-CT_Std	7.11 ± 2.80	6.56 (3.32-12.09)[a]	< 0.05
	Mcro-CT_HI	7.17 ± 2.78	6.63 (3.47-12.1)[a]	
	CBCT_Std	4.80 ± 2.27	4.29 (1.96-8.86)[b]	
	CBCT_HI	4.81 ± 2.25	4.35 (1.99-8.86)[b]	
Structure model index (SMI)	Micro-CT_Std	2.11 ± 0.47[a]	2.22 (1.34-2.91)	< 0.05
	Mcro-CT_HI	2.13 ± 0.48[a]	2.23 (1.35-2.94)	
	CBCT_Std	1.06 ± 0.25[b]	1.11 (0.66-1.48)	
	CBCT_HI	1.08 ± 0.25[b]	1.12 (0.66-1.48)	

[a,b,c,d]: Values in the same column with different superscripts show statistically significant differences for each variable ($P < 0.05$).

ume (BV) was defined as the total volume of trabecular bone within the volume of interest (VOI), and tissue volume (TV) was defined as the total volume of the medullary VOI. As well as serving as the reference for the percentage of volume, TV is a meaningful parameter in its own right. Responses to experimental treatments can include changes in the medullary volume (e.g., from expansion of the endocortical boundary). Percent bone volume (BV/TV) referred to the occupancy of trabecular bone in the medullary VOI. Trabecular thickness (TbTh) was defined as the average thickness of bone trabeculae, trabecular separation (TbSp) as the average separation of trabecular bone, and trabecular number (TbN) as a measure of spatial density (mean number of trabeculae crossed per mm of transect through the VOI). The trabecular bone pattern factor (TbPf), which is also known as the surface convexity index under general scientific nomenclature, measured the ratio of convex (higher values) to concave (lower values) surface curvature. High connectivity between trabeculae causes lower (or more negative) values of this parameter, as does porosity. The

structure model index (SMI), a method intended for determining the plate- or rod-like geometry of trabecular structures, used the change in surface area (BS, from the isosurface) as the volume increased infinitesimally. The SMI is 0 for plates, 3 for rods, and 4 for solid spheres.

Statistical analysis

In order to determine the required minimum sample size, the following criteria were applied: error (α) = 0.05, power (1-b) = 0.80, f = 0.25, and predicted correlation between repeated measurements = 0.75. The Cohen f statistic was used, as it is the appropriate effect size index for analysis of variance (ANOVA). A medium prior effect size (0.25) was used, as proposed by Cohen.[21] It was calculated that 12 (twelve) samples would be sufficient for the study. Stata version 16.1 (StataCorp, College Station, TX, USA) was used for statistical analysis. The statistical significance level was set at $P < 0.05$.

Descriptive statistics for each variable were calculated and presented as mean ± standard deviation (SD). One-way repeated-measures ANOVA and the Friedman test were used to test differences between paired measurements. The Bonferroni test and Dunn test were used as *post hoc* procedures when a significant effect was observed. Intraclass correlation coefficients (ICCs) based on a 2-way mixed-effects model were used to evaluate the consistency and agreement of paired measurements. The ICC values were interpreted as follows: <0.5 as poor reliability; between 0.5 and 0.75 as moderate reliability; between 0.75 and 0.9 as good reliability; and >0.90 as excellent reliability.

Results

Table 1 shows the mean ± SD, minimum, and maximum measurements of BV, BV/TV, BS, TbTh, TbSp, TbN, TbPf, and SMI at different voxel sizes (Std and HI) in both imaging modalities (micro-CT and CBCT). The BV, BV/TV, and TbTh values were higher for CBCT images than for micro-CT images, whereas the BS, TbSp, TbN, TbPf, and SMI values were lower in CBCT images than in micro-CT

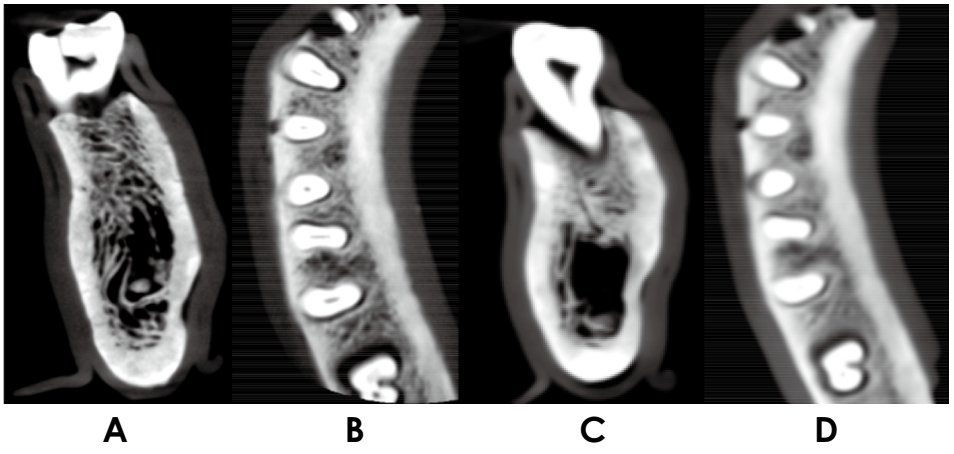

Fig. 1. Cone-beam computed tomographic (CBCT) images before 3-dimensional analysis. A and B. CBCT_HI images. C and D. CBCT_Std images.

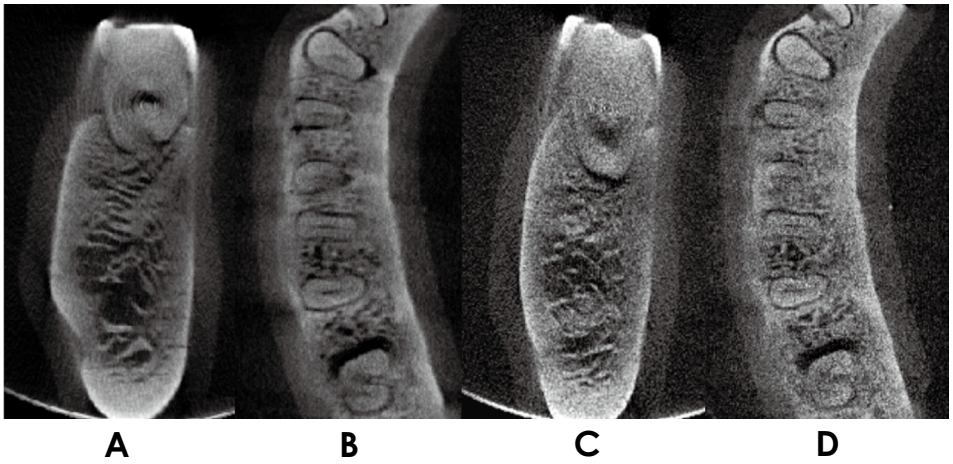

Fig. 2. Micro-computed tomographic (CT) images before 3-dimensional analysis. A and B. Micro-CT_HI images. C and D. Micro-CT_Std images.

Table 2. Assessment of consistency and absolute agreement between measurements

Paired variables	Consistency		Absolute agreement	
	ICC	95% confidence interval	ICC	95% confidence interval
Bone volume (BV)	0.998	0.995-0.999	0.986	0.894-0.997
Percent bone volume (BV/TV)	0.983	0.959-0.995	0.894	0.466-0.973
Bone surface (BS)	0.985	0.963-0.995	0.898	0.471-0.974
Trabecular thickness (TbTh)	0.983	0.960-0.995	0.575	0.081-0.861
Trabecular separation (TbSp)	0.853	0.646-0.953	0.846	0.637-0.95
Trabecular number (TbN)	0.958	0.898-0.986	0.771	0.233-0.936
Trabecular pattern factor (TbPf)	0.993	0.983-0.998	0.926	0.534-0.982
Structure model index (SMI)	0.960	0.903-0.987	0.560	0.069-0.852

ICC: intraclass correlation coefficient

Table 3. Compatibility between micro-CT and CBCT at standard and high resolutions

	Paired variables	Consistency		Absolute agreement	
		ICC	95% confidence interval	ICC	95% confidence interval
Standard micro-CT vs. CBCT	Bone volume (BV)	0.993	0.975-0.998	0.959	0.008-0.993
	Percent bone volume (BV/TV)	0.971	0.900-0.992	0.734	0.077-0.946
	Bone surface (BS)	0.952	0.833-0.986	0.738	0.135-0.945
	Trabecular thickness (TbTh)	0.95	0.825-0.985	0.302	0.022-0.742
	Trabecular separation (TbSp)	0.597	−0.399-0.884	0.586	0.318-0.878
	Trabecular number (TbN)	0.859	0.510-0.959	0.483	0.154-0.852
	Trabecular pattern factor (TbPf)	0.979	0.927-0.994	0.81	0.081-0.964
	Structure model index (SMI)	0.881	0.585-0.966	0.279	0.052-0.718
High micro-CT vs. CBCT	Bone volume (BV)	0.994	0.979-0.998	0.961	0.006-0.993
	Percent bone volume (BV/TV)	0.943	0.803-0.984	0.755	0.170-0.948
	Bone surface (BS)	0.956	0.849-0.987	0.743	0.125-0.947
	Trabecular thickness (TbTh)	0.953	0.836-0.986	0.308	0.021-0.748
	Trabecular separation (TbSp)	0.525	0.351-0.863	0.512	0.235-0.855
	Trabecular number (TbN)	0.89	0.619-0.968	0.531	0.140-0.875
	Trabecular pattern factor (TbPf)	0.978	0.923-0.994	0.801	0.082-0.962
	Structure model index (SMI)	0.879	0.581-0.965	0.282	0.053-0.721

CT: computed tomography, CBCT: cone-beam computed tomography, ICC: intraclass correlation coefficient

images. In both imaging methods, the BV, BV/BT, TbTh, and TbSp variables showed higher values when Std voxels were used than when HI voxels were used, whereas the BS, TbPf, and SMI variables had higher values for HI voxels than for Std voxels. BV, BS, and TbTh were statistically significantly different for each imaging method and voxel size ($P<0.05$). TbN, TbPf, and SMI were statistically significantly different between imaging methods ($P<0.05$). Different CBCT and micro-CT images before the 3D analysis are shown in Figures 1 and 2.

The ICCs and confidence intervals (CIs) of all measurements obtained for different voxels (Std and HI) with different methods (micro-CT and CBCT) are presented in Table 2. All variables showed high-level consistency among the paired measurements, whereas the absolute agreement for TbTh and SMI were moderate and the rest of the variables ranged from good to excellent. The absolute agreement for TbTh and SMI was moderate, while the absolute agreement between the other variables was good or excellent.

The agreement between the different voxel sizes (Std and HI) is presented in Table 3. TbSp had a moderate level of consistency, whereas the other variables had good to ex-

Table 4. Agreement between standard (Std) and high (HI) resolutions for micro-CT and CBCT

Paired variables		Consistency		Absolute agreement	
		ICC	95% confidence interval	ICC	95% confidence interval
Micro-CT Std vs. HI	Bone volume (BV)	1	0.998-1	1	0.970-1
	Percent bone volume (BV/TV)	0.997	0.991-0.999	0.987	0.349-0.998
	Bone surface (BS)	0.999	0.998-1	0.998	0.867-1
	Trabecular thickness (TbTh)	0.997	0.989-0.999	0.988	0.494-0.998
	Trabecular separation (TbSp)	0.999	0.996-1	0.996	0.802-0.999
	Trabecular number (TbN)	0.999	0.995-1	0.999	0.995-1
	Trabecular pattern factor (TbPf)	1	0.999-1	1	0.997-1
	Structure model index (SMI)	0.999	0.998-1	0.999	0.995-1
CBCT Std vs. HI	Bone volume (BV)	1	0.999-1	0.999	0.971-1
	Percent bone volume (BV/TV)	0.983	0.942-0.995	0.971	0.780-0.993
	Bone surface (BS)	0.999	0.996-1	0.996	0.766-0.999
	Trabecular thickness (TbTh)	0.999	0.997-1	0.994	0.380-0.999
	Trabecular separation (TbSp)	0.998	0.991-0.999	0.994	0.852-0.999
	Trabecular number (TbN)	0.996	0.985-0.999	0.996	0.986-0.999
	Trabecular pattern factor (TbPf)	1	0.999-1	1	0.999-1
	Structure model index (SMI)	0.996	0.987-0.999	0.995	0.981-0.999

ICC: intraclass correlation coefficient

cellent consistency. Considering the absolute agreement, BV was excellent; TbPf was good; BV/TV and BS were moderate, while the other variables (TbTh, TbN, and SMI) showed poor agreement.

The agreement between different imaging methods (micro-CT and CBCT) is presented in Table 4. All variables showed excellent consistency and absolute agreement.

Discussion

In the present study, the usefulness of CBCT in the evaluation of trabecular bone structure was investigated using morphometric parameters. A possible explanation of why CBCT overestimated BV, BV/TV and TbTh when compared to micro-CT may be its low resolution.[22] More specifically, thin trabeculae appear thicker when there is low image resolution. The high spatial resolution of micro-CT was considered to be of paramount importance for accurately evaluating trabecular structure. This may explain the low absolute agreement between CBCT and micro-CT for some parameters that were found to be overestimated or underestimated when compared to micro-CT.[23] A correction factor can be calculated in order to reduce bias in overestimates. Despite the small number of bone samples, this study demonstrated the potential of high-resolution CBCT imaging for quantitative bone morphometry and bone quality assessment.

The morphological analysis of bone structure in clinical practice was found to be reliable with advances in CBCT resolution. Especially in implant dentistry, 3D images obtained using CBCT have emerged as an accurate diagnostic modality and reliable planning tool.[10] Retrospective clinical studies regarding the relationship between bone parameters and implant stability may help develop new classification systems and study protocols related to bone structure. The indication for CBCT scanning depends on the physician's preference; however, unnecessary use of CBCT scans should be avoided, as they have higher radiation doses and costs than 2D images. It is recommended that an optimal small voxel size and the smallest FOV available should be utilized to improve diagnostic quality and reduce patient exposure.[24]

Dental implants are mainly in contact with trabecular bone, which contributes directly to implant stability.[25,26] Today, CBCT is routinely used before dental implant surgery.[26-28] Studies have shown that BV/TV, which represents the ratio of trabecular bone volume to tissue volume, is the most important parameter for determining bone quality.[29,30] In addition, some other studies found that BV/TV and bone density were related to each other.[12,31] According to our findings, CBCT and micro-CT measurements are very compatible considering the BV/TV parameter. Some

other studies found higher BV/TV, TbTh, and TbSp values and lower TbN values using CBCT when compared to micro-CT.[27,32,33] Another study found positive correlations between BV/TV, BS/TV, TbTh, TbN, and bone density measurements.[34] Pauwels et al.[35] investigated the effects of exposure parameters and voxel size on the analysis of bone structures using 20 posterior mandibular samples and found no significant difference for BV/TV. However, TbTh and TbSp were affected by different voxel sizes.

Previous micro-CT and histology studies demonstrated that the morphometric parameters of trabecular bone structure had a significant correlation with the physical structure of the bone.[7,36,37] Although this study was performed in the absence of motion and object artifacts originating from surrounding anatomical structures, such as the tongue or vertebra,[20] human jawbones along with a soft tissue equivalent were used to simulate real clinical situations. The presence of metallic materials in the oral cavity in normal clinical settings is quite common, but samples with restorative materials that could cause artifacts[20] were not used in this study.

The deviation of the CBCT measurements in the study from the gold standard might be due to the increased scattering amount, noise level, and artifacts unique to the scanner technology.[20] A higher noise level may result in more inconsistencies in voxels' gray values.[38,39] In this study, a fully automated and observer-independent 3D matching algorithm was used for recording micro-CT and CBCT scans. All measurements were made in the same region, ensuring voxel accuracy. However, there was a possibility of observer error and selection of different regions due to the manual alignment of CBCT and micro-CT datasets. Finally, the difference in voxel size between CBCT (0.2 mm, 0.075 mm) and micro-CT (0.12 mm, 0.06 mm) might also have contributed to inconsistencies in the calculated parameters.

Image quality is affected by several factors, such as voxel size, the unit itself, tube voltage, and FOV selection.[40] Generally, smaller voxel sizes enable higher spatial resolution and provide sharper images of the oral region. However, small voxels require a higher radiation exposure dose.[41] The smaller voxel sizes of CBCT increase the noise levels when compared to micro-CT, due to the low tube voltage, cone beam deflection, and low detector efficiency.[42] Different voxel sizes in CBCT may lead to comparable diagnostic results in the visibility of hard tissue such as bone.[43] Although the possible effect of varying voxel sizes on cancellous bone measurements was demonstrated in micro-CT, it is not known whether this applies to different voxel sizes in CBCT. In this study, the screening protocols recommended by the manufacturer were followed. Image quality was optimized, but the results were limited to a single CBCT device and results may show discrepancies with other devices.[44] Future generalization of research findings can be supported by the use of innovative CBCT systems and technical standards.

Within the limitation of this *ex vivo* study, the trabecular microstructure of the mandible was investigated using CBCT and micro-CT devices. These findings may not always be applicable to real conditions, as *ex vivo* samples may differ from *in vivo* samples in terms of the bone microstructure pattern and molecular concentration. Despite the mean differences in morphometric parameters, the observations of good consistency and absolute agreement values between different parameters in micro-CT and CBCT imaging show the potential of high-resolution CBCT imaging for *in vivo* applications. High-resolution CBCT offers an ideal and reliable alternative to determine the 3D trabecular bone structure in the preoperative stage. Thus, the location of dental implants may be determined during clinical applications, and a drill protocol related to the bone type can be developed for endosseous implants according to classifications based on measurable density.[45]

Conflicts of Interest: None

References

1. Fuh LJ, Huang HL, Chen CS, Fu KL, Shen YW, Tu MG, et al. Variations in bone density at dental implant sites in different regions of the jawbone. J Oral Rehabil 2010; 37: 346-51.
2. Lioubavina-Hack N, Lang NP, Karring T. Significance of primary stability for osseointegration of dental implants. Clin Oral Implants Res 2006; 17: 244-50.
3. Fyhrie DP. Summary - measuring "bone quality". J Musculoskelet Neuronal Interact 2005; 5: 318-20.
4. Ozan O, Turkyilmaz I, Yilmaz B. A preliminary report of patients treated with early loaded implants using computerized tomographyguided surgical stents: flapless versus conventional flapped surgery. J Oral Rehabil 2007; 34: 835-40.
5. Muller R. Bone microarchitecture assessment: current and future trends. Osteoporos Int 2003; 14 Suppl 5: S89-95.
6. Diederichs G, Link TM, Kentenich M, Schwieger K, Huber MB, Burghardt AJ, et al. Assessment of trabecular bone structure of the calcaneus using multi-detector CT: correlation with microCT and biomechanical testing. Bone 2009; 44: 976-83.
7. Parfitt AM, Mathews CH, Villanueva AR, Kleerekoper M, Frame B, Rao DS. Relationships between surface, volume, and thickness of iliac trabecular bone in aging and in osteoporosis. Implications for the microanatomic and cellular mechanisms of bone loss. J Clin Invest 1983; 72: 1396-409.
8. Müller R, Van Campenhout H, Van Damme B, Van Der Perre G, Dequeker J, Hildebrand T, et al. Morphometric analysis of

human bone biopsies: a quantitative structural comparison of histological sections and micro-computed tomography. Bone 1998; 23: 59-66.
9. Hsu JT, Chen YJ, Tsai MT, Lan HHC, Cheng FC, Chen MY, et al. Predicting cortical bone strength from DXA and dental cone-beam CT. PLoS One 2012; 7: e50008.
10. Benavides E, Rios HF, Ganz SD, An CH, Resnik R, Reardon GT, et al. Use of cone beam computed tomography in ımplant dentistry: the International Congress of Oral Implantologists consensus report. Implant Dent 2012; 21: 78-86.
11. Nackaerts O, Maes F, Yan H, Couto Souza P, Pauwels R, Jacobs R. Analysis of intensity variability in multislice and cone beam computed tomography. Clin Oral Implants Res 2011; 22: 873-9.
12. González-García R, Monje F. The reliability of cone-beam computed tomography to assess bone density at dental implant recipient sites: a histomorphometric analysis by micro-CT. Clin Oral Implants Res 2013; 24: 871-9.
13. Kothari M, Keaveny TM, Lin JC, Newitt DC, Genant HK, Majumdar S. Impact of spatial resolution on the prediction of trabecular architecture parameters. Bone 1998; 22: 437-43.
14. Issever AS, Link TM, Kentenich M, Rogalla P, Burghardt AJ, Kazakia GJ, et al. Assessment of trabecular bone structure using MDCT: comparison of 64- and 320- slice CT using HR-pQCT as the reference standard. Eur Radiol 2010; 20: 458-68.
15. Naitoh M, Katsumata A, Mitsuya S, Kamemoto H, Ariji E. Measurement of mandibles with microfocus X-ray computerized tomography and compact computerized tomography for dental use. Int J Oral Maxillofac Implants 2004; 19: 239-46.
16. Lou L, Lagravere MO, Compton S, Major PW, Flores-Mir C. Accuracy of measurements and reliability of landmark identification with computed tomography (CT) techniques in the maxillofacial area: a systematic review. Oral Surg Oral Med Oral Pathol Oral Radiol Endod 2007; 104: 402-11.
17. Liu S, Zhang ZY, Li JP, Liu DG, Ma XC. A study of trabecular bone structure in the mandibular condyle of healthy young people by cone beam computed tomography. Zhonghua Kou Qiang Yi Xue Za Zhi 2007; 42: 357-60.
18. Corpas Ldos S, Jacobs R, Quirynen M, Huang Y, Naert I, Duyck J. Peri-implant bone tissue assessment by comparing the outcome of intra-oral radiograph and cone beam computed tomography analyses to the histological standard. Clin Oral Implants Res 2011; 22: 492-9.
19. Hua Y, Nackaerts O, Duyck J, Maes F, Jacobs R. Bone quality assessment based on cone beam computed tomography imaging. Clin Oral Implants Res 2009; 20: 767-71.
20. Schulze R, Heil U, Gross D, Bruellmann DD, Dranischnikow E, Schwanecke U, et al. Artefacts in CBCT: a review. Dentomaxillofac Radiol 2011; 40: 265-73.
21. Cohen J. Statistical power analysis for the behavioral sciences. 2nd ed. Hillsdale, NJ: Erlbaum; 1988. p. 285-7.
22. Waarsing JH, Day JS, Weinans H. An improved segmentation method for in vivo microCT imaging. J Bone Miner Res 2004; 19: 1640-50.
23. Bohner L, Tortamano P, Gremse F, Chilvarquer I, Kleinheinz J, Hanisch M. Assessment of trabecular bone during dental ımplant planning using cone-beam computed tomography with high-resolution parameters. Open Dent J 2021; 15: 57-63.
24. Vandenberghe B, Luchsinger S, Hostens J, Dhoore E, Jacobs R, SEDENTEXCT Project Consortium. The influence of exposure parameters on jawbone model accuracy using cone beam CT and multislice CT. Dentomaxillofac Radiol 2012; 41: 466-74.
25. Kang SR, Bok SC, Choi SC, Lee SS, Heo MS, Huh KH, et al. The relationship between dental implant stability and trabecular bone structure using cone-beam computed tomography. J Periodontal Implant Sci 2016; 46: 116-27.
26. Ibrahim N, Parsa A, Hassan B, van der Stelt P, Aartman IH, Wismeijer D. Accuracy of trabecular bone microstructural measurement at planned dental implant sites using cone-beam CT datasets. Clin Oral Implants Res 2014; 25: 941-5.
27. Kim JE, Yi WJ, Heo MS, Lee SS, Choi SC, Huh KH. Three-dimensional evaluation of human jaw bone microarchitecture: correlation between the microarchitectural parameters of cone beam computed tomography and micro-computer tomography. Oral Surg Oral Med Oral Pathol Oral Radiol 2015; 120: 762-70.
28. Panmekiate S, Ngonphloy N, Charoenkarn T, Faruangsaeng T, Pauwels R. Comparison of mandibular bone microarchitecture between micro-CT and CBCT images. Dentomaxillofac Radiol 2015; 44: 20140322.
29. Parsa A, Ibrahim N, Hassan B, van der Stelt P, Wismeijer D. Bone quality evaluation at dental implant site using multislice CT, micro-CT, and cone beam CT. Clin Oral Implants Res 2015; 26: e1-7.
30. Parfitt AM, Drezner MK, Glorieux FH, Kanis JA, Malluche H, Meunier PJ, et al. Bone histomorphometry: standardization of nomenclature, symbols, and units: report of the ASBMR Histomorphometry Nomenclature Committee. J Bone Miner Res 1987; 2: 595-610.
31. Naitoh M, Hirukawa A, Katsumata A, Ariji E. Prospective study to estimate mandibular cancellous bone density using large volume cone-beam computed tomography. Clin Oral Implants Res 2010; 21: 1309-13.
32. Kulah K, Gulsahi A, Kamburoğlu K, Geneci F, Ocak M, Celik HH, et al. Evaluation of maxillary trabecular microstructure as an indicator of implant stability by using 2 cone beam computed tomography systems and micro-computed tomography. Oral Surg Oral Med Oral Pathol Oral Radiol 2019; 127: 247-56.
33. Van Dessel J, Huang Y, Depypere M, Rubira-Bullen I, Maes F, Jacobs R. A comparative evaluation of cone beam CT and micro-CT on trabecular bone structures in the human mandible. Dentomaxillofac Radiol 2013; 42: 20130145.
34. Monje A, Monje F, González-García R, Galindo-Moreno P, Rodriguez-Salvanes F, Wang HL. Comparison between micro-computed tomography and cone-beam computed tomography radiologic bone to assess atrophic posterior maxilla density and microarchitecture. Clin Oral Implants Res 2014; 25: 723-8.
35. Pauwels R, Faruangsaeng T, Charoenkarn T, Ngonphloy N, Panmekiate S. Effect of exposure parameters and voxel size on bone structure analysis in CBCT. Dentomaxillofac Radiol 2015; 44: 20150078.
36. Chappard D, Retailleau-Gaborit N, Legrand E, Baslé MF, Audran M. Comparison insight bone measurements by histomorphometry and microCT. J Bone Miner Res 2005; 20: 1177-84.
37. de Oliveira RC, Leles CR, Lindh C, Ribeiro-Rotta RF. Bone tissue microarchitectural characteristics at dental implant sites.

Part 1: identification of clinical-related parameters. Clin Oral Implants Res 2012; 23: 981-6.
38. Aranyarachkul P, Caruso J, Gantes B, Schulz E, Riggs M, Dus I, et al. Bone density assessments of dental implant sites: 2. Quantitative cone-beam computerized tomography. Int J Oral Maxillofac Implants 2005; 20: 416-24.
39. Araki K, Okano T. The effect of surrounding conditions on pixel value of cone beam computed tomography. Clin Oral Implants Res 2013; 24: 862-5.
40. Kamburoğlu K, Murat S, Kolsuz E, Kurt H, Yüksel S, Paksoy C. Comparative assessment of subjective image quality of cross-sectional cone-beam computed tomography scans. J Oral Sci 2011; 53: 501-8.
41. Davies J, Johnson B, Drage N. Effective doses from cone beam CT investigation of the jaws. Dentomaxillofac Radiol 2012; 41: 30-6.
42. Hassan B, Couto Souza P, Jacobs R, de Azambuja Berti S, van der Stelt P. Influence of scanning and reconstruction parameters on quality of three-dimensional surfaces models of the dental arches from cone beam computed tomography. Clin Oral Investig 2010; 14: 303-10.
43. Spin-Neto R, Gotfredsen E, Wenzel A. Impact of voxel size variation on CBCT-based diagnostic outcome in dentistry: a systemic review. J Digit Imaging 2013; 26: 813-20.
44. De Vos W, Casselman J, Swennen GR. Cone-beam computerized tomography (CBCT) imaging of the oral and maxillofacial region: a systematic review of the literature. Int J Oral Maxillofac Surg 2009; 38: 609-25.
45. Misch CE. Bone classification, training keys to implant success. Dent Today 1989; 8: 39-44.